land

Article

The Effects of Climate Change on Habitat Connectivity: A Case Study of the Brown-Eared Pheasant in China

An Cao [1] and Xueyi Shi [1,2,3,*]

[1] School of Land Science and Technology, China University of Geosciences, Beijing 100083, China; 2112200036@cugb.edu.cn
[2] Key Laboratory of Land Consolidation and Rehabilitation, Ministry of Natural Resources, Beijing 100035, China
[3] Technology Innovation Center for Ecological Restoration in Mining Areas, Ministry of Natural Resources, Beijing 100083, China
* Correspondence: shixueyi60@cugb.edu.cn

Abstract: Climate change has caused habitat fragmentation and reduced connectivity. The Fen River Basin in Shanxi Province, China is an important habitat for the central population of the brown-eared pheasant (BEP). The effects of climate change need to be considered in the conservation planning of BEP habitats. We used a species dispersion model to determine the BEP core habitat and graph theory to explore the connectivity of the BEP's main habitats. The pinch point areas of BEP dissemination were determined by circuit theory. Least-cost pathways were used to identify the critical corridors for BEP dissemination. A gap analysis was conducted to estimate the efficiency of BEP conservation measures. Under the future climate scenarios, BEP habitats decreased by between 54.69% and 97.63%, and the connectivity of the main habitats was reduced by a similar magnitude. The BEP core habitat shifted to the southwestern region under the influence of climatic conditions. Currently, 90.84% of the species' critical habitat remains unprotected. Due to climate change, the core habitat in the future was projected to differ from the current protected area. Enhancing the protection of the pinch point region may aid in the restoration of habitat connectivity.

Keywords: climate change; future climate scenarios; brown-eared pheasant; habitat connectivity; gap analysis

check for updates

Citation: Cao, A.; Shi, X. The Effects of Climate Change on Habitat Connectivity: A Case Study of the Brown-Eared Pheasant in China. *Land* **2022**, *11*, 806. https://doi.org/10.3390/land11060806

Academic Editors: Baojie He, Ayyoob Sharifi, Chi Feng and Jun Yang

Received: 25 April 2022
Accepted: 27 May 2022
Published: 29 May 2022

1. Introduction

Climate change will cause changes in biological phenology, species richness, and the geographic distribution of species [1]. Without effective mitigation and conservation measures, many species will be at risk of extinction [2]. In particular, endangered species that are sensitive to the climate are most vulnerable to climate change [3]. Therefore, it is essential to conserve vulnerable species under climate change to maintain a specific habitat scale and good habitat connectivity.

Crossoptilon mantchuricum, a member of the Galliformes, Phasianidae, *Crossoptilon*, is a rare bird that is endemic to China. It mainly inhabits mixed coniferous and broadleaf forests at altitudes of 1000 to 2600 m. It is one of the most important wildlife species in China, and the International Union for Conservation of Nature (IUCN) Red List also lists it as a vulnerable species.

Numerous studies on the habitat and population size of the brown-eared pheasant (BEP) have been conducted. During the overwintering and breeding periods, the BEP population is distributed in a clustered pattern over a large scale [4]. The selection of spring foraging sites by the BEP is mainly related to food, concealment, and water sources [5]. When choosing a wintering habitat, the BEP mainly seeks small areas with a local abundance of food after a secluded environment is identified at a large scale [6]. In addition, changes in the BEP habitat over time and under future climatic scenarios have also attracted the attention of researchers.

According to historical data, the region with appropriate habitats for the BEP diminishes as forest cover decreases [7]. Li [8] predicted the potential range of the BEP in the 2050s and 2070s under several climatic scenarios. Frequent human disturbance, such as overhunting and tourist development, were among the BEP's primary threats [9,10]. Meanwhile, the BEP was very susceptible to land-use change and habitat degradation [11]. Previous studies have shown that the BEP has an apparent habitat selectivity. The survival and development of their populations are extremely sensitive to climate conditions.

Future global climate change and the resulting changes in habitat quality may impact the distribution and survival of the BEP. Although some researchers [8,12,13] have studied the potential habitats of the BEP under climate change, further research on potential changes in habitat connectivity is needed.

In this study, the distribution records of the BEP in the Fen River Basin were compiled and the MaxEnt model was used to determine the geographical area that is currently suitable for the BEP. We predicted the potential distribution of the BEP and its habitat connectivity in the Fen River Basin under future climate scenarios. The future trends in the species' geographic distribution and dispersal pathways were predicted. The conservation effectiveness of nature reserves for the BEP in the watershed was assessed to provide a reference for long-term conservation measures in response to climate change.

2. Methods

The framework for assessing changes in the BEP habitat suitability and connectivity, identifying pinch points, and gap analysis is shown in Figure 1.

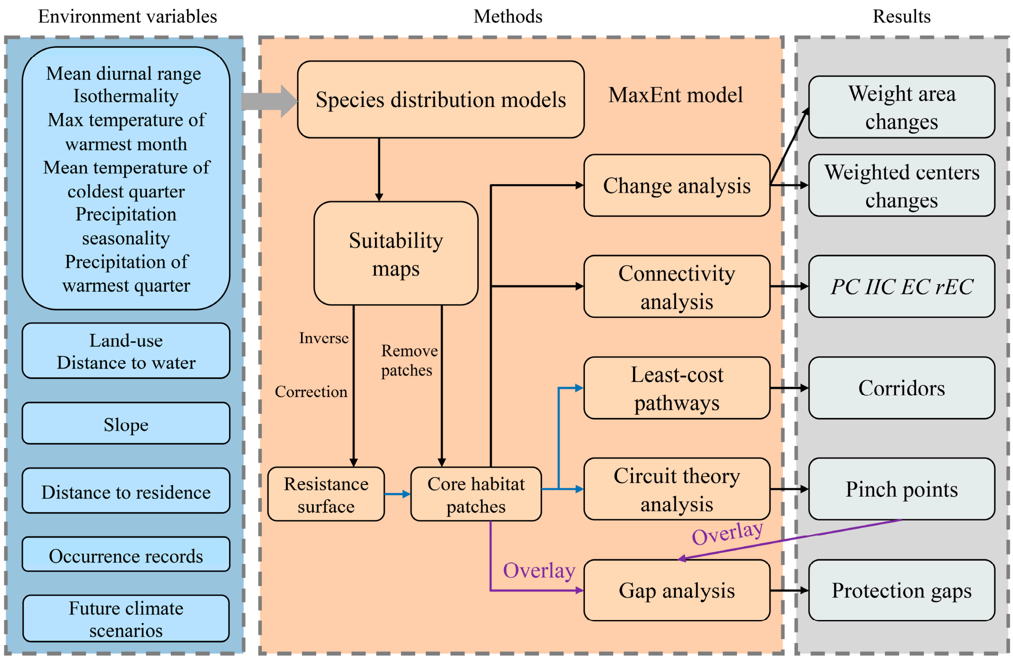

Figure 1. The framework for assessing changes in the BEP habitat suitability and connectivity, identifying pinch points, and gap analysis.

2.1. Study Area

The Fen River Basin is situated in Shanxi Province's middle and southern regions in Figure 2. The basin is bounded on the east by the Yunzhong Mountains, Taihang Mountains, and the Haihe River; on the west by the Luya Mountains, Lüliang Mountains, and the Yellow River's north mainstream; on the southeast by the Taiyue Mountains and the Qin River; and on the south by the Qin River. The dimensions of the basin are 413 km from north to south, 188 km from east to west, and the mainstream is 716 km long.

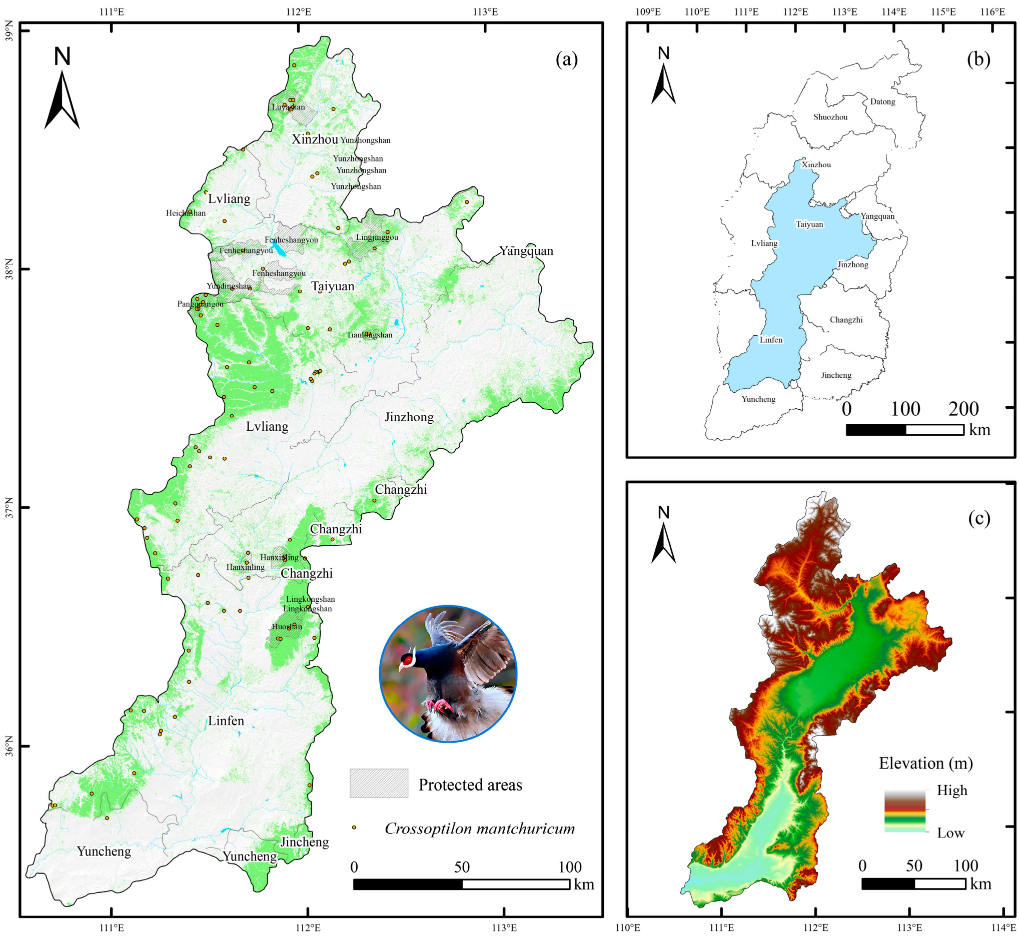

(a) Occurrences of the brown-eared pheasant in the study area and nature reserves for the protection of the brown-eared pheasant

(b) Location of the study area in Shanxi Province

(c) Elevation of the study area

Figure 2. Location of the Fen River Basin, BEP record points, and the elevation.

The 39,492 km^2 study area includes the two main distribution areas of the BEP in Shanxi Province. In the traditional distribution area, the BEP is continuously distributed along the ridgeline of the Lüliang Mountains, and the other major distribution area is the forest land in the Taiyue Mountains [12]. The BEP was originally found in the Taiyue Mountains but did not spread from the Lüliang Mountains to the Taiyue Mountains [12].

There are 11 nature reserves in the Fen River Basin for the protection of the BEP, including 4 national nature reserves and 7 provincial nature reserves. Numerous nature reserves are located in the northwest of the Fen River Basin along the Lüliang Mountains, while a few are scattered in the central part of the basin.

Brown-eared pheasant occurrence records were obtained from the global biodiversity information facility (GBIF, https://www.gbif.org/ accessed on 10 May 2022), eBird (https://ebird.org/ accessed on 10 May 2022), BirdReport (http://www.birdreport.cn/ accessed on 10 May 2022), and the available literature [7,12] see Supplementary Materials. Occurrences without clear coordinates were removed. Forests, conservation stations, villages, and towns included in each nature reserve of the BEP were found based on the geographical names database to find their central latitude and longitude [8]. In addition, we also compiled recent reports of BEP on the Internet and confirmed their specific coordinates through Google Earth (https://earth.google.com/ accessed on 10 May 2022). The BEP record reports were selected according to the following principles: (1) only data from exclusively within the research region were used; (2) duplicate points and other points within 300 m were removed to minimize model overfitting [13]; (3) points that fell outside the species' height range were removed [14]; (4) only one point position was kept in a grid cell to avoid the effect of spatial autocorrelation as much as possible [15]; and (5) all points need to meet the physiological conditions of BEP to some extent. The global Moran I index was calculated to test whether the occurrence data are aggregated.

2.2. Environmental Variables

Suitable environmental variables were selected based on a comprehensive consideration of the ecological, life history, and biological characteristics of the BEP [4–6]. Habitat factors such as vegetation, elevation, climate, and anthropogenic disturbance all have an effect on habitat selection of the BEP [13,14].

We classified environmental elements into four categories while developing species distribution models (SDMs) for the BEP: climate, habitat, terrain, and human influences. The climate data were CMIP6 downscaled future climate projections derived from WorldClim 2.1 (www.worldclim.org accessed on 17 December 2021) [16]. We used the common delta method to downscale the climate data [17]. The scale of change of the future climate scenario from the base period was calculated, and the measured data of the base period were multiplied by this scale and then interpolated to 300 m [18]. Habitat environmental variables include land-use and distance to water. Land-use in the current period was derived from ESA Worldcover (www.esa-worldcover.org accessed on 28 December 2021); however, if the projection used the current land-use type, it may affect the overall accuracy. Future land-use changes based on four shared socioeconomic pathways (SSPs) were used to predict future habitat changes in the BEP [19]. We obtained the distance to water by calculating the Euclidean distance to a river or lake. Terrain variables include elevation and slope. GDEMV3 30-m digital elevation data collected from the Geospatial Data Cloud were used to determine the elevation and slope (www.gscloud.cn accessed on 15 December 2021). Human influences variables include distance to roads and distance to residence. The same treatment as for water was applied to roads, towns, and rural. The water, roads, towns, and rural vector maps were obtained from the National Catalogue Service for Geographic Information (www.webmap.cn accessed on 8 December 2021). The resolution of all environmental variables was unified to 300 m. Selected environmental factors were filtered to reduce the effect of covariate relationships between variables [20]. We eliminated variables with correlation coefficients greater than 0.8 [21].

2.3. Different Future Climate Scenarios

We used the Beijing Climate Center climate system model version 2 (BCC-CSM2-MR), with four SSPs (126, 245, 370, and 585). The BCC-CSM2-MR was suitable for East Asia and had been extensively studied [22]. To study the response of the BEP to climate change, we selected climate data for the periods of 2020–2040 (2030s) and 2040–2060 (2050s).

2.4. Species Distribution Models

The Maxent model can effectively deal with complex environment variables with collinearity, and over-parameterization has less impact on the model than a lack of parameterization [23,24]. We created SDMs for the BEP based on occurrence data and the environmental variables. The SDMs were created with the Maxent (v 3.4.4) (https://biodiversityinformatics.amnh.org/open_source/maxent/ accessed on 5 November 2021) program. The training set contained 75% of the random sample points, and the test set contained 25% of the random sample points. A total of 10,000 pseudo-absence points were randomly generated, the maximum number of iterations was 500, and the model was run 10 times to obtain robust results [25]. The area under the curve (AUC) of the receiver operating characteristic curve values showed a great advantage in the performance assessment of the SDMs [26,27]. Cohen's Kappa was also an important metric to consider when evaluating models [28]. Omission rate (OR) was the percentage of abnormal samples not correctly classified in the test sample compared to the total number of abnormal samples in the test sample, and a smaller value indicates higher prediction accuracy [29]. Generally, 0.5 < AUC < 1, with the maximum value of 1 representing the theoretically most accurate model.

2.5. Habitat Change Assessment

The 10% training presence logistic threshold (10% TPLT) ensures the smallest omission rate, and, for habitat assessments, it is appropriate to include at least 90% of the total known sample points. This value is frequently used in threshold selection [7,30]. We set less than 10% TPLT as a low suitability. We set a TPLT of less than 10% as low fitness. Habitats with low suitability will be treated as non-habitats. Empirically, we used 0.6 as the threshold to distinguish between moderate and high suitability [14]. The home area of the BEP ranges from 2 to 128 ha [31]. All patches larger than 2 ha will be used to build a connectivity network [32].

Considering the spatial heterogeneity of habitat distribution, we calculated the weighted area [33,34]. To quantify the change in habitat area, the total weighted areas of all patches were calculated. The sum of grid values within all habitat patches was calculated to obtain the weighted area. Meanwhile, we generated mean values for the latitude and longitude of the weighted centers of all habitat patches to examine the geographic variance in core habitats.

2.6. Habitat Connectivity Estimation

We chose four metrics to measure the habitat connectivity of the BEP, which were calculated by Confor 2.6 (http://www.conefor.org/ accessed on 22 November 2021). The *probability of connectivity* index (*PC*) is commonly used to assess the connectivity among habitats [35]. *PC* may be defined as the chance that two randomly placed animals within a landscape would arrive in habitat patches that are approachable from one another (interconnected) given the set of habitat patches and their connections (p_{ij}) [36]. This index was calculated by Saura et al. [36]:

$$PC = \frac{\sum_{i=1}^{n} \sum_{j=1}^{n} a_i a_j p_{ij}^*}{A_l^2}, \tag{1}$$

where n represents the total number of habitat patches; a_i and a_j signify the weighted habitat area of patches I and j, respectively; p_{ij}^* denotes the species' greatest dispersion probability between patches i and j; and A_l signifies the weighted habitat area of the total study area, including habitat and non-habitat patches. We selected the maximum dispersal distance of the BEP and set the probability value to 0.05 in Confor 2.6 [37]. *PC* is a numeric number between 0 and 1, with 0 suggesting that species are not biologically related between habitat patches and 1 representing the optimal connection.

The *integral index of connectivity (IIC)* is similar to *PC*, but it also assesses the dispersion possibilities between habitat units [38]. Rather than using dispersion probabilities, *IIC* employs a binary connection model in which two habitat units are either related or not. This index was calculated by Pascual-Hortal et al. [38]:

$$IIC = \frac{\sum_{i=1}^{n} \sum_{j=1}^{n} \frac{a_i \cdot a_j}{1+nl_{ij}}}{A_l^2} \tag{2}$$

where nl_{ij} denotes the number of links in the shortest path (topological distance) connecting patches i and j; the meanings of the other variables are the same as in Equation (1).

An *equivalent connectivity area* (*ECA*) is defined as the size of a single habitat patch (maximally connected) that would have the same probability of connection as the landscape's current habitat pattern [39]. We chose a weighted habitat area rather than area, and, therefore, we referred to this index as *EC*. This index was calculated by Saura et al. [39]:

$$EC = \sqrt{\sum_{i=1}^{n} \sum_{j=1}^{n} a_i a_j p_{ij}^*} \tag{3}$$

the variables are the same as in Equation (1).

Following a certain spatial change in the landscape, the relative variation in *EC* may be directly compared to the variation in the total amount of weighted habitat area in the landscape after the same change [35]. This index was calculated by Dilts et al. [33]:

$$rEC = \frac{dEC}{dWA} \tag{4}$$

where *dEC* and *dWA* denote relative changes of *EC* and weighted area, respectively.

rEC is larger than 1 when the habitat alteration results in a disproportionate change in connectivity; otherwise, this value is less than 1. A score of less than 1 indicates that the connection has shifted as a result of random habitat changes [34].

2.7. Least-Cost pathways

We used the inverse of suitability as the friction layer, which avoids the subjective opinions of experts, which is more advantageous [40].

Linkage Mapper 3.0 (https://linkagemapper.org/ accessed on 22 November 2021) was used to simulate least-cost pathways and extract habitat corridors. The tool creates a cost-weighted distance (CWD) surface by calculating the CWD of each grid cell from the nearest source, then calculates the least CWD and simulates the least-cost pathway. It removes least-cost paths between perfectly adjacent habitat patches and least-cost paths that exceed the farthest dispersal distance [31].

2.8. Circuit Theory Analysis

Circuit theory reflects the relative importance of habitat patches and corridors using the strength of currents between core habitats. Circuit theory may be used to forecast the movement patterns and chance of dispersion or death of random walkers traversing complicated environments [41]. It can be used to connect habitat patches and determine key corridors for conservation planning.

Circuitscape 4.0 software (https://circuitscape.org/ accessed on 22 November 2021) models connectivity based on circuit theory. It is widely used in the identification of animal corridors because the electronic charges can travel randomly, similar to the animal movement process [42]. We used the pairwise mode in the Pinchpoint Mapper tool to create a circuit density map and identify pinch points.

2.9. Gap Analysis

We obtained vector maps of the nature reserves in the study area from the Resource and Environment Science and Data Center (www.resdc.cn accessed on 7 November 2021). The vector maps were overlaid on the core habitat patches in the current period to assess the proportion of protected area to habitat and the proportion of different suitability areas within the protected areas. Areas with a high current density were considered to be important pathways for BEP dispersal. The vector maps were overlaid on the current density maps under future climate scenarios to assess the conservation efficiency of protected areas for important habitat patches.

3. Results

3.1. Habitat Suitability Variation

After removing the highly relevant environment variables, the 12 variables include mean diurnal range (bio2), isothermality (bio3), max temperature of warmest month (bio5), mean temperature of coldest quarter (bio11), precipitation seasonality (bio15), precipitation of warmest quarter (bio18), precipitation of coldest quarter (bio19), land-use, distance to water, slope, distance to road, and distance to residence. The Moran index of the occurrence point was calculated as follows: 0.176, z = 2.37, p = 0.007. The AUC values for all the SDMs were higher than 0.8 in all the climate scenarios, the Kappa was higher than 0.7, and the OR was less than 0.05, so the results were plausible in Table 1.

Table 1. Evaluation metrics of SDM for BEP.

Period	AUC	Omission Rate	Cohen's Kappa
current	0.89	0.02	0.75
2030 SSP126	0.87	0.01	0.76
2030 SSP245	0.89	0.03	0.80
2030 SSP370	0.89	0.02	0.82
2030 SSP585	0.88	0.05	0.81
2050 SSP126	0.88	0.02	0.76
2050 SSP245	0.88	0.03	0.75
2050 SSP370	0.87	0.02	0.79
2050 SSP585	0.89	0.04	0.80

Among all the environmental variables, land-use showed a large dominance, with a mean contribution of about 27.45%. The contribution of bio5 was 17.77% to 20.83%, ranking second in Table 2. The contributions of "distance to water", "distance to roads", and "slope" were all below 5% or even lower in Table 2. Land-use change and anthropogenic disturbance have a greater impact on BEP habitat than climate change.

Table 2. Variable contribution of SDM for BEP.

Period	Bio2	Bio3	Bio5	Bio11	Bio15	Bio18	Bio19	Land-Use	Distance to Water	Slope	Distance to Road	Distance to Residence
current	4.92	3.55	20.48	2.12	10.62	12.57	5.86	26.33	0.94	3.82	2.59	6.19
2030SSP126	6.16	3.47	19.44	1.72	10.85	13.31	3.20	27.14	0.80	4.65	3.22	6.04
2030SSP245	5.20	4.08	20.09	1.63	10.56	12.03	5.41	28.80	0.64	3.81	2.81	4.94
2030SSP370	6.60	3.69	20.33	2.01	10.65	11.55	5.19	27.66	1.20	2.76	3.05	5.31
2030SSP585	4.63	3.34	18.43	1.42	10.20	9.16	11.78	28.11	0.80	2.37	3.45	6.30
2050SSP126	3.87	3.46	18.87	1.21	8.62	8.27	16.03	27.69	0.88	4.12	2.34	4.64
2050SSP245	4.57	4.17	17.77	1.28	9.72	8.35	14.23	27.54	0.58	3.56	3.66	4.56
2050SSP370	5.02	3.57	20.83	1.86	10.84	11.29	6.65	26.64	0.90	4.44	2.45	5.50
2050SSP585	4.26	2.95	20.82	2.03	9.81	12.39	6.73	27.20	1.08	3.03	2.82	6.88

The 10% training presence logistic thresholds of different climate scenarios were shown in Table 3. All the 10% TPLT were basically stable at around 0.27, with the highest value not exceeding 0.30.

Table 3. The 10% training presence logistic threshold of different climate scenarios.

Period	10% Training Presence Logistic Threshold
current	0.27
2030 SSP126	0.27
2030 SSP245	0.26
2030 SSP370	0.29
2030 SSP585	0.26
2050 SSP126	0.30
2050 SSP245	0.26
2050 SSP370	0.27
2050 SSP585	0.30

After removing the small patches, the weighted area of the existing suitable habitat was 86,810.10 in Figure 3a. Moderately suitable habitat accounted for 37.95% of the study area, whereas highly suitable habitat accounted for 34.92%.

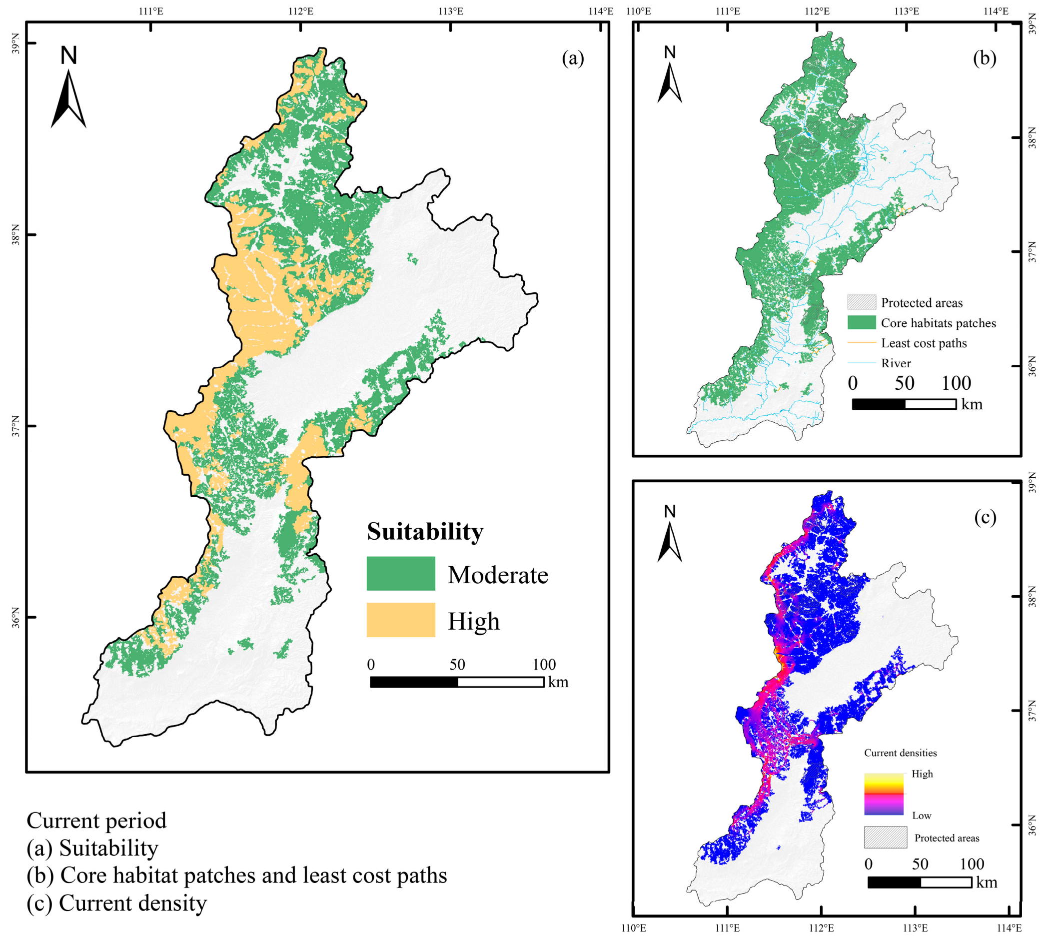

Figure 3. Suitability map, core habitat patches map, and current density map for the current period.

The outputs of the MaxEnt model were reclassified according to different suitability thresholds to obtain suitability classification maps in Figure 4. After vectorizing these maps, patches with an area less than 2 ha were excluded to obtain the core habitats of BEP in Figure 5.

The weighted area of the different periods is shown in Figure 6. Although the range of suitable habitats varied among the SSPs, the proportion of suitable habitats was lower in all the future climate scenarios than in the current period. The 2050s SSP585 had the most significant reduction in weighted area (97.63%). With just a 54.69% decrease in weighted area, the 2030s SSP585 experienced the least loss in weighted area.

Under future climate scenarios, the weighted area of suitable habitats was much greater in the 2030s SSP245 and SSP585 than in the other scenarios. The weighted area of highly suitable habitat for the 2030s SSP126 and 2050s SSP585 scenarios, account for about 0.81% of the total weighted area. Under the four different 2030 climate scenarios, the weighted area of suitable habitats accounted for 22.32%, 63.16%, 25.97%, and 57.34%, respectively, of the basin in Figure 6. Under the four climate scenarios for the 2050s, the weighted area of suitable habitats accounted for 41.53%, 45.68%, 34.21%, and 12.93%, respectively, of the basin in Figure 6.

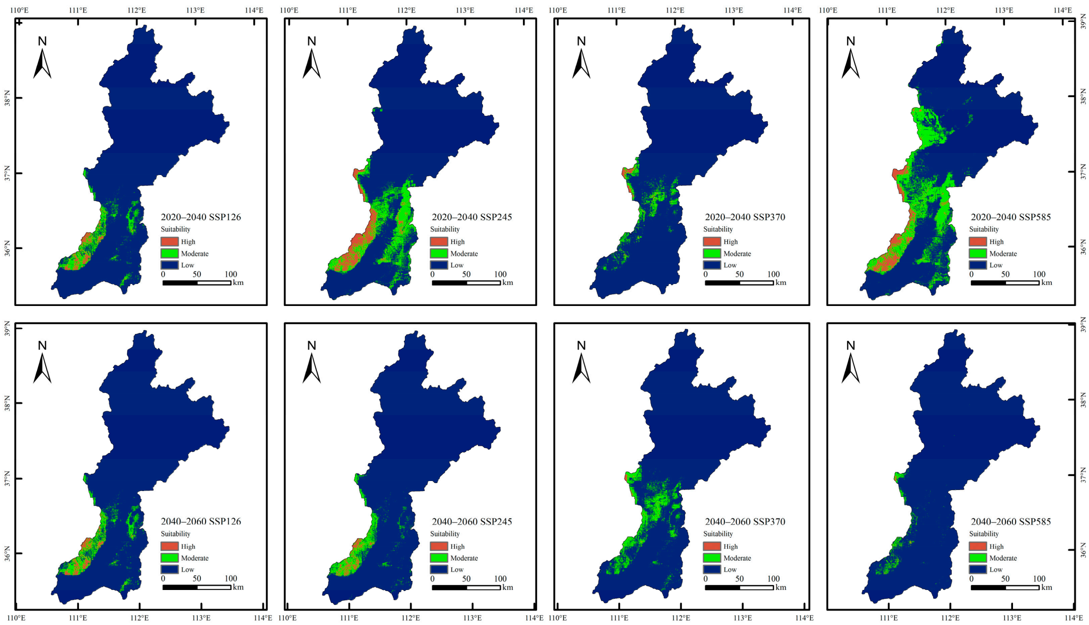

Figure 4. The suitability maps of all climate scenarios.

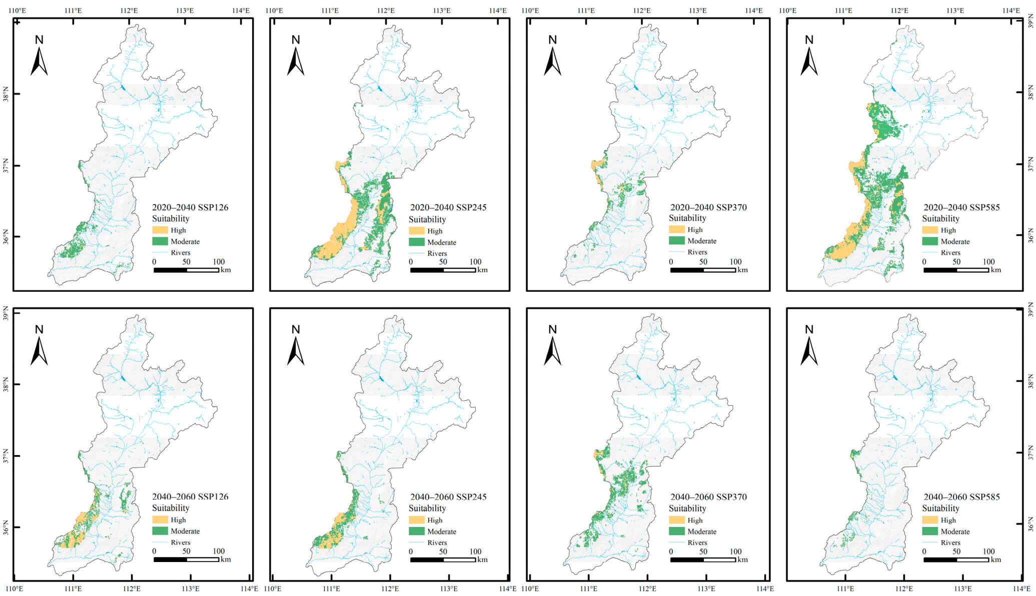

Figure 5. Distribution of suitable habitats in the future scenarios.

We assessed the spatial variation in habitats by calculating the weighted centroids of all the habitat patches and averaging them in Figure 7. The current latitude of the core habitat patches was 37.04° and the longitude was 111.77°. In all the future scenarios, there was a shift in the habitat from the present position to the south. The transfer distance ranged from a minimum of 57 km (2030s SSP585) to a maximum of 117 km (2050s SSP245). The latitude of the core habitat patches stabilized at 36.13° in the 2030s SSP126, 2050s SSP126, 2050s SSP245, and 2050s SSP585; 36.23° in the 2030s SSP245; 36.42° in the 2050s SSP370; and 36.55° in the 2030s SSP370 and SSP585. The longitude of the core habitat patches stabilized at 111.13° in the 2050s SSP585; 111.21° in the 2050s SSP245; 111.34° in the 2030s SSP126, 2050s SSP126; 111.45° in the 2030s SSP370, 2050s SSP370; and 111.54° in the 2030s SSP245 and SSP585.

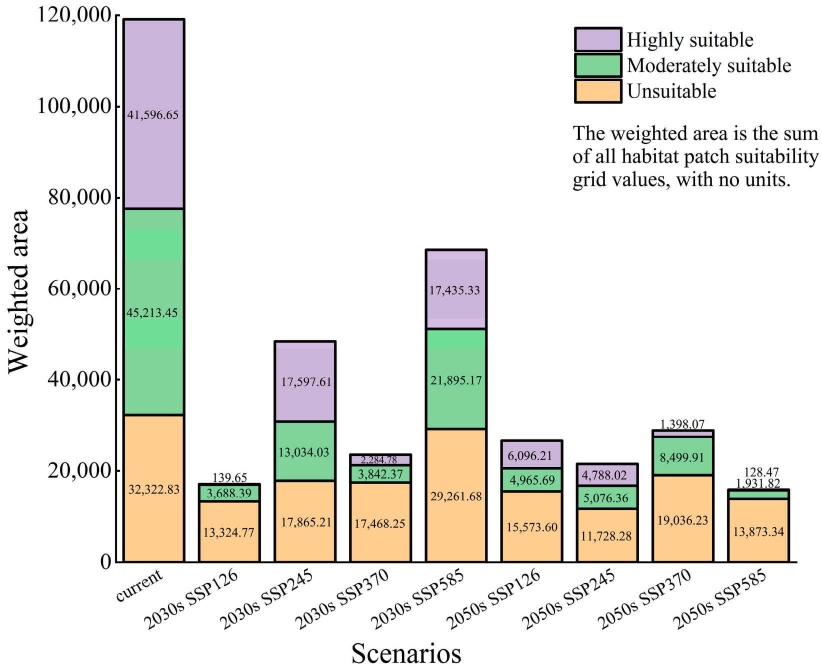

Figure 6. The weighted area of all periods.

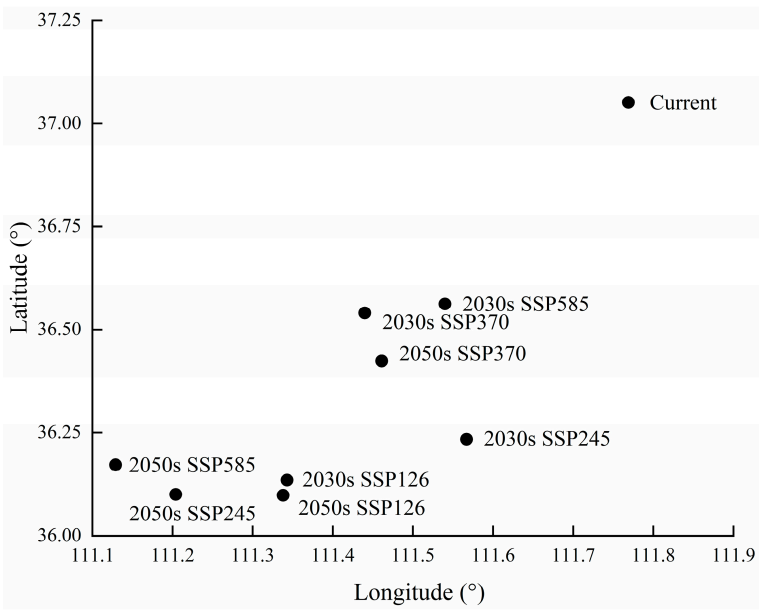

Figure 7. Spatial variation in the weighted centroids of habitats in all periods.

3.2. Habitat Connectivity Variation

Table 4 shows the calculation results of the connectivity metrics. The values of *PC*, *IIC*, and *EC* for the future climate scenarios were all lower than the current values. For *PC*, the difference between the maximum (2030s SSP245) and minimum (2050s SSP585) is more than 100 times. For *IIC*, the difference between the maximum (2030s SSP245) and minimum (2050s SSP585) is nearly 60 times. The 2030s SSP245 climate scenario showed the best connectivity. 2030s SSP585, which has the largest equivalent connectivity, has the second-best connectivity after 2030s SSP245. The connectivity of 2050s SSP585 is weaker than the others in all the climate scenarios.

Table 4. The connectivity indicators.

Time	*PC*	*IIC*	*EC*	*rEC*
Current	0.519	0.218	85,271.14	
2020–2040				
SSP126	0.021	0.019	2,497.71	1.02
SSP245	0.331	0.175	27,833.29	1.04
SSP370	0.014	0.011	2780.14	1.02
SSP585	0.298	0.173	37,108.97	1.03
2040–2060				
SSP126	0.125	0.065	9,406.96	1.01
SSP245	0.174	0.088	8,963.01	1.02
SSP370	0.042	0.024	5,887.12	1.05
SSP585	0.003	0.003	876.25	1.01

The *rEC* values for all eight future climate scenarios were slightly greater than 1. The *rEC* values suggested that the loss of habitat was essentially equal to the loss of connectivity.

After excluding the least-cost pathways between completely adjacent habitat patches and least-cost paths that exceed the farthest dispersal distance, 57 corridors were identified in the current period, as shown in Figure 3b. These corridors are mainly located in areas where the habitat edges are heavily fragmented. Figure 8 shows the least-cost pathways between the core habitat patches for the different future climate scenarios. The largest number of corridors was identified in the 2030s SSP585 scenario, with 157 corridors. These corridors were mainly located in the northern, central, and southeast of the basin, connecting a large number of fragmented habitat patches. The minimum number of corridors identified in the 2050s SSP245 scenario was 45. These corridors were mainly distributed in the habitat patch fragmentation area southwest of the study area.

Currently, the areas with a high current density are mainly distributed along the Lüliang Mountain Range, and we discovered a total of 20 pinch points, as shown in Figure 3c. The current densities varied significantly between the climate scenarios, as shown in Figure 9. An area of high current density was distributed in the southwest of the basin in 2030s SSP126 and 2050s SSP126, SSP245, and SSP585. A moderate current density was spread in the middle of the basin in 2030s SSP245, SSP370, and SSP585 and 2050s SSP370. As a necessary route for BEP dispersal, the pinch point areas with high current density were crucial areas that need to be protected to enhance the habitat connectivity.

3.3. Gap Analyses

Within the region studied, there were 11 nature reserves with a total area of 1496.98 km^2 that serve to preserve the BEP. Patches of BEP habitat were found in all the nature reserves, as seen in Figure 3b. Within the Fen River Basin, the extent of the protected areas is much smaller than the extent of suitable habitats. Currently, 90.84% of the BEP habitat patches remain unprotected in the study area. Figure 3c shows that the Luyashan National Nature Reserve and three provincial nature reserves (Fenheshangyou Nature Reserve, Yundingshan Nature Reserve, and Hanxinling Nature Reserve) had relatively high current densities. The only one with a high current density in the 2030s and 2050s was Hanxinling Provincial Nature Reserve. In Figure 10, suitable habitats in the central part of the watershed are covered by protected areas only under the 2030SSP245, 2030SSP370, 2030SSP585, and 2050SSP370 scenarios. Suitable habitats in other areas are not covered by protected areas. Figure 11 shows the different suitabilities of the nature reserves at the present time. Under the climate scenarios, Hanxinling Provincial Nature Reserve and Huoshan Provincial Nature Reserve both had locations with a reasonably high current density (Figure 9) for both 2030s SSP245 and 2030s SSP585.

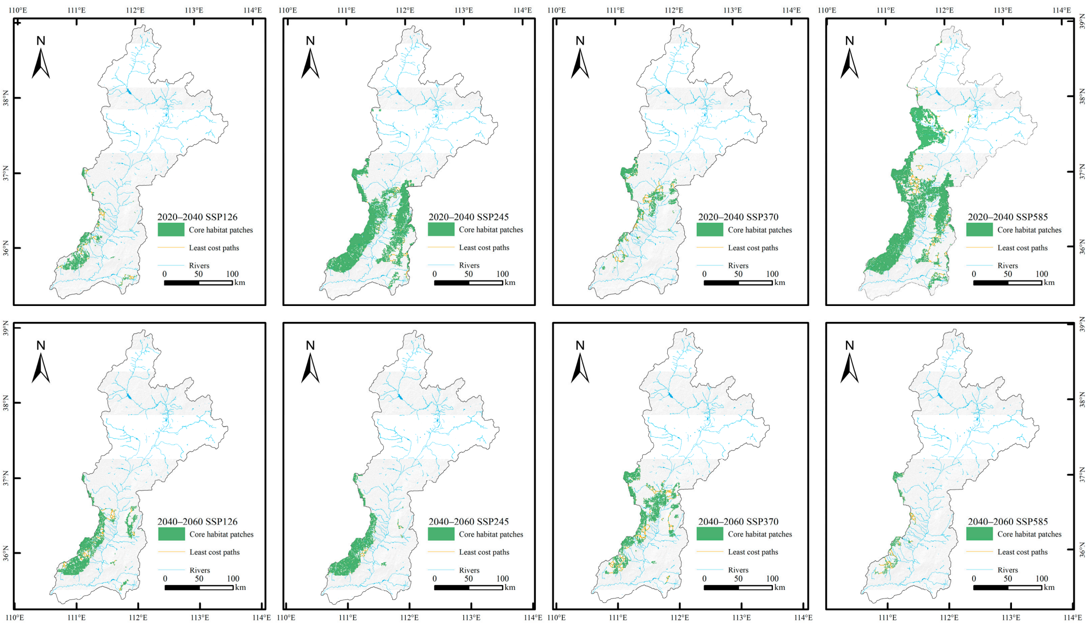

Figure 8. Core habitat patches maps and least-cost pathway maps for the different climate scenarios.

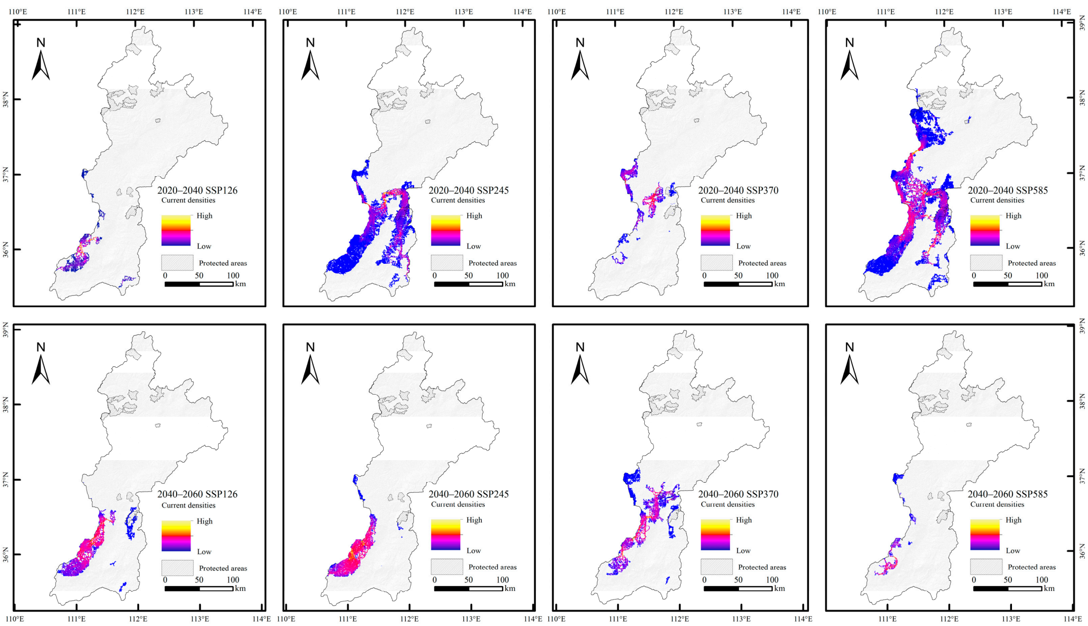

Figure 9. Current density maps of different climate scenarios.

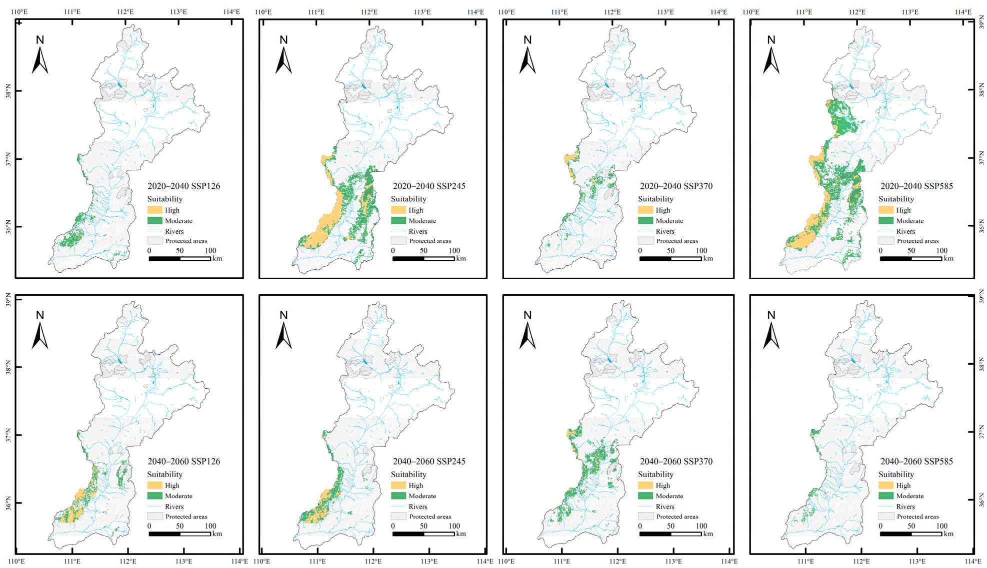

Figure 10. The proportion of different suitability in the protected areas at the present time.

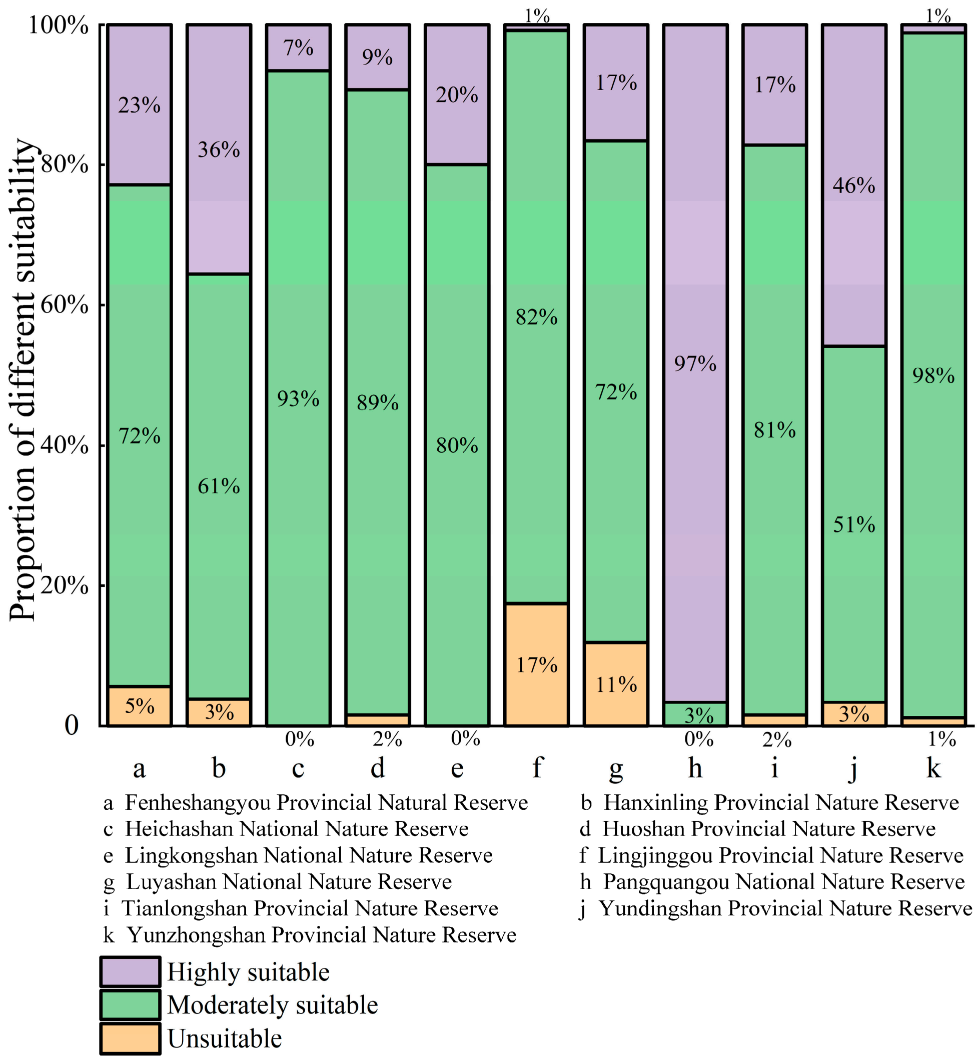

Figure 11. The proportion of different suitability in the nature reserves at the present time.

4. Discussion

4.1. Habitat Suitability Area Variation

The area of suitable habitat for the BEP in the Fen River Basin decreased under all the climate scenarios in the 2030s and 2050s. In the current period, our results were in line with those of previous studies in terms of predicting the suitable distribution range of the BEP in the basin [8,13,15]. The current suitable habitat of the BEP was found to be greater than that reported by Li [14]. This may be related to the policy of returning farmland to forest in China and the decrease in agricultural population. Highly suitable habitats were distributed closer to the edge of the study area than moderately suitable habitats. The high suitability habitat is farther from the edge of the forest areas, which may help to reduce anthropogenic disturbance or provide effective protection against natural enemies. Conservation measures for the BEP, therefore, require further attention [43].

However, the suitable range of the BEP habitat under future climate scenarios differed from that reported by Li [8]. The climate data selected by Li were from CMIP5. This difference may be related to the choice of climate data, with the CMIP6 model coupling more anthropogenic effects on climate than the CMIP5 model [44]. There was also a difference in the threshold for habitat suitability, with a 10% TPLT being used in the present study. The different thresholds may be an essential reason for the variation in the suitable area. Based on the results, it is clear that the impact of land-use change on BEP habitats may be greater than climate change. Coupling climate change and anthropogenic land-use may be more effective in predicting habitat change. Land-use change accounted for a significant proportion of the contribution of all the environmental variables. Our results also suggested that the suitable habitat for the BEP will shift to the southwest in the future. The shift in the location of the suitable habitat may also be an important reason for the reduction in the suitable habitat in the Fen River Basin under future scenarios.

4.2. Habitat Suitability Spatial Variation

The study showed that the habitat of BEP shifted under the influence of climate, which is consistent with Young's prediction [12]. The core habitat of BEP shifts to the southwest, which may be related to the distribution of *Pinus tabuliformis. Pinus tabuliformis* forests are ideal habitats for BEP, which eat the seeds of *Pinus tabuliformis* and are effectively protected from natural predators in the forests [45]. The altitude of the BEP distribution area in the Taiyue Mountains is only about 500 m, all lower than other areas [12]. The low altitude area of the Taiyue Mountains is covered with a large number of mixed coniferous and broadleaf forests, as well as mixed forests of trees and shrubs, which provide rich food for the BEP [13].

4.3. Habitat Connectivity

Habitat connectivity is crucial for species dispersal. The construction of resistance surfaces plays a vital role in assessing the connectivity of habitat patches [46]. Combining the surface landscape with the areas of anthropogenic disturbance to determine the extent of the resistance surface is one method to determine the connectivity [32]. Using the inverse of suitability as the resistance surface effectively reduces the subjectivity in determining the resistance value [33,34].

Under future climate scenarios, the habitat may become highly fragmented and even unsuitable. The results showed that the loss of habitat connectivity may be as serious as the loss of habitat, and we should, therefore, be concerned about both the loss of habitat patches and the reduction in connectivity [39]. The Taiyue Mountains forest area and Lüliang Mountains forest area are separated by the Fen River valley. The habitat in this area is severely fragmented and not well covered with forest vegetation. Habitat patches in this area were clearly fragmented in the 2030s SSP245, SSP370, and SSP585 and 2050s SSP370. It would, therefore, be difficult for the BEP to move into this area, which was consistent with the results of Yang [12]. There were multiple least-cost pathways and a relatively high current density in this area, making it an important area for BEP diffusion. The dispersal of the BEP could be effectively promoted by protecting the pinch point area. The results of our study provide theoretical guidance for building the integrity and connectivity of the BEP habitat.

At present, the high current density in nature reserves, such as Pangquangou, we speculate, may be related to two factors: (1) the ecological conditions in the nature reserves are better and are important patches for BEP to spread or inhabit; (2) the presence of captive populations in the nature reserves may cause high current density. However, with climate change, the core habitat shifts, and the nature reserves may need to reselect the boundary in the future as well.

4.4. Gap Analysis

The nature reserves protecting the BEP in the Fen River basin are mainly located along the Lüliang Mountains and are concentrated in the middle and upper parts of the basin. There are also nature reserves in the central part of the basin, as well as in the Taiyue Mountains. Some populations are still active outside of the nature reserves. Most of the suitable habitat for the BEP is located in about 90.84% of the area not currently covered by nature reserves, and this observation was consistent with Li et al. [14]. Under future climate scenarios, the suitable habitats were projected to shift to the southwest and were not within the existing nature reserves. Therefore, the scope of the reserves should be expanded, and the boundaries of the protected areas should be redefined as a conservation measure.

5. Conclusions

Our study shows that the connectivity of the BEP habitat in the Fen River Basin has significantly decreased as a consequence of climate change. In addition, the reduction in the habitat will result in an equal degree of loss in connectivity. Therefore, it will be important to enhance the connectivity conservation in the pinch point area. In addition, we found a conservation gap between the current distribution of the BEP and the existing nature reserves in the Fen River Basin. With climate change, the shift in the BEP habitats to the southwest will further widen the conservation gap. Management measures to adjust the scope of protected areas and strengthen the protection of pinch point areas will help to bridge the conservation gap. The distribution area of the central population of the BEP is not only in the Fen River Basin, although our findings can only be applied to the Fen River Basin. We suggest that the scope of the study area should be expanded in future studies to include the central population of the BEP and enhance the overall connectivity. In future work, we can construct ensemble species distribution models to reduce the error of single-species distribution models. Many habitats in some areas have different suitability categories but are spatially connected, and the impact of their connectivity on the overall habitat connectivity should be considered.

Supplementary Materials: The following supporting information can be downloaded at: https://www.mdpi.com/article/10.3390/land11060806/s1, Table S1: Longitude and latitude recorded by the brown-eared pheasant.

Author Contributions: Conceptualization, A.C.; methodology, A.C.; software, A.C.; validation, A.C.; formal analysis, A.C.; investigation, A.C.; resources, A.C.; data curation, A.C.; writing—original draft preparation, A.C.; writing—review and editing, A.C.; visualization, A.C.; supervision, X.S.; project administration, X.S.; funding acquisition, X.S. All authors have read and agreed to the published version of the manuscript.

Funding: This research was funded by Charity Special Project of Ministry of Land and Resources People's Republic of China, grant number 201411007.

Data Availability Statement: The data used to support the findings of this study are available from the authors upon request.

Acknowledgments: We thank all reviewers for their valuable comments on this paper.

Conflicts of Interest: The authors declare no conflict of interest.

References

1. Pecl, G.T.; Araujo, M.B.; Bell, J.D.; Blanchard, J.; Bonebrake, T.C.; Chen, I.C.; Clark, T.D.; Colwell, R.K.; Danielsen, F.; Evengard, B.; et al. Biodiversity redistribution under climate change: Impacts on ecosystems and human well-being. *Science* **2017**, *355*, eaai9214. [CrossRef] [PubMed]
2. Thomas, C.D.; Cameron, A.; Green, R.E.; Bakkenes, M.; Beaumont, L.J.; Collingham, Y.C.; Erasmus, B.F.; De Siqueira, M.F.; Grainger, A.; Hannah, L.; et al. Extinction risk from climate change. *Nature* **2004**, *427*, 145–148. [CrossRef] [PubMed]
3. Pacifici, M.; Visconti, P.; Butchart, S.H.M.; Watson, J.E.M.; Cassola, F.M.; Rondinini, C. Species' traits influenced their response to recent climate change. *Nat. Clim. Chang.* **2017**, *7*, 205–208. [CrossRef]
4. Zhang, G.G.; Zhang, Z.W.; Zheng, G.M. Spatial pattern and habitat selection of brown eared pheasant in Wulushan Nature Reserve, Shanxi Province. *Biodivers. Sci.* **2003**, *11*, 303–308. [CrossRef]
5. Li, H.Q.; Lian, Z.M.; Chen, C.G. Feeding-Sites Selection of Brown Eared Pheasant in Spring in Huanglong Mountains, Shaanxi Province. *Chi. J. Zool.* **2007**, *42*, 61–67.
6. Zhang, G.G.; Zheng, G.M.; Zhang, Z.W. Scale-dependent wintering habitat selection by brown-eared pheasant in Luyashan Nature Reserve of Shanxi, China. *Acta Ecol. Sin.* **2005**, *25*, 952–957.
7. Li, Y.L.; Li, X.; Song, Z.; Ding, C. Determining the distribution loss of brown eared-pheasant (Crossoptilon mantchuricum) using historical data and potential distribution estimates. *PeerJ* **2016**, *4*, e2556. [CrossRef]
8. Li, H.Q.; Han, P.S.; Niu, C.H. Impact of Climate Change on the Potential Habitat of Brown-Eared Pheasant (Crossoptilon mantchuricum), An Endemic and Endangered Animals to China. *Sci. silvae sin.* **2021**, *57*, 102–110.
9. Guan, Z.M. Resource status and conservation measures of the Brown Eared Pheasant in Heichashan Nature Reserve. *For. Shanxi* **2012**, *6*, 34–35.
10. Ren, Q.L.; Li, J.F. Survival, research status and conservation measures of the brown eared pheasant. *Spec Econ. anim. Plants* **2020**, *23*, 4–5; +7.
11. Song, K.; Mi, C.R.; Yang, N.; Sun, L.; Sun, Y.H.; Xu, J.L. Improve the roles of nature reserves in conservation of endangered pheasant in a highly urbanized region. *Sci. Rep.* **2020**, *10*, 17673. [CrossRef] [PubMed]
12. Yang, X.M. Distribution of Crossoptilon mantchuricum in Shanxi Province. *Chin. J. Wildl.* **2020**, *41*, 1085–1090. [CrossRef]
13. Li, H.Q.; Niu, C.H.; Han, P.S. Study on the Suitable Habitat of Western Population of Brown-Eared Pheasent Crossoptilon mantchuricum Based on MaxEnt Model. *J. Ecol. Rural. Environ.* **2020**, *36*, 499–504.
14. Li, Y.L.; Cui, B.; Qiu, X.; Ding, C.; Batool, I. Management reference for nature reserve networks based on MaxEnt modeling and gap analysis: a case study of the brown-eared pheasant in China. *Anim. Biodiv. Conserv.* **2016**, *39*, 241–252. [CrossRef]
15. Shcheglovitova, M.; Anderson, R.P. Estimating optimal complexity for ecological niche models: A jackknife approach for species with small sample sizes. *Ecol. Model.* **2013**, *269*, 9–17. [CrossRef]
16. Fick, S.E.; Hijmans, R.J. WorldClim 2: new 1-km spatial resolution climate surfaces for global land areas. *Int. J. Climatol.* **2017**, *37*, 4302–4315. [CrossRef]
17. Zhao, F.F.; Xu, Z.X. Comparative analysis on downscaled climate scenarios for headwater catchment of yellow river using SDS and DELTA methods. *Cata. meteorol. sin.* **2007**, *65*, 653–662.
18. Liu, Q.; Gao, L.; Ma, M.M.; Wang, L.; Lin, H. Downscaling of temperature and precipitation in the Daling River Basin, Liaoning Province. *Water Resour. and Hydropower Eng.* **2021**, *52*, 16–31. [CrossRef]
19. Liao, W.L.; Liu, X.P.; Xu, X.Y.; Chen, G.Z.; Liang, X.; Zhang, H.H.; Li, X. Projections of land use changes under the plant functional type classification in different SSP-RCP scenarios in China. *Sci. Bull.* **2020**, *65*, 1935–1947. [CrossRef]
20. Xu, Z.L.; Peng, H.H.; Peng, S.Z. The development and evaluation of species distribution models. *Acta Ecol. Sin.* **2015**, *35*, 557–567.
21. Brown, J.L. SDMtoolbox: a python-based GIS toolkit for landscape genetic, biogeographic and species distribution model analyses. *Methods Ecol. Evol.* **2014**, *5*, 694–700. [CrossRef]
22. Wu, T.W.; Lu, Y.X.; Fang, Y.J.; Xin, X.G.; Li, L.; Li, W.P.; Jie, W.H.; Zhang, J.; Liu, Y.M.; Zhang, L.; et al. The Beijing Climate Center Climate System Model (BCC-CSM): the main progress from CMIP5 to CMIP6. *Geosci. Model Dev.* **2019**, *12*, 1573–1600. [CrossRef]
23. Kong, W.Y.; Li, X.H.; Zou, H.F. Optimizing MaxEnt model in the prediction of species distribution. *Ying Yong Sheng Tai Xue Bao* **2019**, *30*, 2116–2128. [CrossRef] [PubMed]
24. Elith, J.; Phillips, S.J.; Hastie, T.; Dudik, M.; Chee, Y.E.; Yates, C.J. A statistical explanation of MaxEnt for ecologists. *Divers. Distrib.* **2011**, *17*, 43–57. [CrossRef]
25. Barbet-Massin, M.; Jiguet, F.; Albert, C.H.; Thuiller, W. Selecting pseudo-absences for species distribution models: how, where and how many? *Methods Ecol. Evol.* **2012**, *3*, 327–338. [CrossRef]
26. Raes, N.; ter Steege, H. A null-model for significance testing of presence-only species distribution models. *Ecography* **2007**, *30*, 727–736. [CrossRef]
27. Jiménez-Valverde, A. Insights into the area under the receiver operating characteristic curve (AUC) as a discrimination measure in species distribution modelling. *Glob. Ecol. Biogeogr.* **2012**, *21*, 498–507. [CrossRef]
28. Mouton, A.M.; De Baets, B.; Goethals, P.L.M. Ecological relevance of performance criteria for species distribution models. *Ecol. Model.* **2010**, *221*, 1995–2002. [CrossRef]
29. Phillips, S.J.; Anderson, R.P.; Schapire, R.E. Maximum entropy modeling of species geographic distributions. *Ecol. Model.* **2006**, *190*, 231–259. [CrossRef]

30. Ye, W.J.; Yang, N.; Yang, B. Impacts of climate change on potential geographical distribution of golden pheasant (Chrysolophus pictus), an endemic species in China. *Chin. J. Ecol.* **2021**, *40*, 1783–1792. [CrossRef]
31. Wang, G.D.; Feng, X.S.; LI, J.Q. A study on the activity zone and dispersal behavior of the Brown Eared-pheasant. In Proceedings of the The Third National Symposium on Wildlife Ecology and Resource Conservation, Shanghai, China, 1 October 2006; p. 17.
32. Wang, M.D.; Liu, J.M.; He, Z. The construction of ecological security pattern in mountain scenic area based on connectivity and sensitivity: A Case study of Yunqiu Mountain in Shanxi Province. *J. Chin. Ecotourism* **2021**, *11*, 266–282.
33. Dilts, T.E.; Weisberg, P.J.; Leitner, P.; Matocq, M.D.; Inman, R.D.; Nussear, K.E.; Esque, T.C. Multiscale connectivity and graph theory highlight critical areas for conservation under climate change. *Ecol. Appl.* **2016**, *26*, 1223–1237. [CrossRef] [PubMed]
34. Liang, J.C.; Ding, Z.F.; Jiang, Z.G.; Yang, X.J.; Xiao, R.B.; Singh, P.B.; Hu, Y.M.; Guo, K.J.; Zhang, Z.X.; Hu, H.J. Climate change, habitat connectivity, and conservation gaps: a case study of four ungulate species endemic to the Tibetan Plateau. *Landsc. Ecol.* **2021**, *36*, 1071–1087. [CrossRef]
35. Keeley, A.T.H.; Beier, P.; Jenness, J.S. Connectivity metrics for conservation planning and monitoring. *Biol. Conserv.* **2021**, *255*, 109008. [CrossRef]
36. Saura, S.; Pascual-Hortal, L. A new habitat availability index to integrate connectivity in landscape conservation planning: Comparison with existing indices and application to a case study. *Landsc. Urban Plan.* **2007**, *83*, 91–103. [CrossRef]
37. Saura, S.; Torné, J. Conefor Sensinode 2.2: A software package for quantifying the importance of habitat patches for landscape connectivity. *Environ. Modell. Softw.* **2009**, *24*, 135–139. [CrossRef]
38. Pascual-Hortal, L.; Saura, S. Comparison and development of new graph-based landscape connectivity indices: towards the priorization of habitat patches and corridors for conservation. *Landsc. Ecol.* **2006**, *21*, 959–967. [CrossRef]
39. Saura, S.; Estreguil, C.; Mouton, C.; Rodriguez-Freire, M. Network analysis to assess landscape connectivity trends: Application to European forests (1990-2000). *Ecol. Indic.* **2011**, *11*, 407–416. [CrossRef]
40. Gherghel, I.; Martin, R.A. Postglacial recolonization of North America by spadefoot toads: integrating niche and corridor modeling to study species' range dynamics over geologic time. *Ecography* **2020**, *43*, 1499–1509. [CrossRef]
41. Mcrae, B.H.; Dickson, B.G.; Keitt, T.H.; Shah, V.B. Using Circuit Theory to Model Connectivity in Ecology, Evolution, and Conservation. *Ecology* **2008**, *89*, 2712–2724. [CrossRef]
42. McRae, B.H.; Shah, V.B.; Mohapatra, T.K. Circuitscape 4 User Guide. Available online: http://www.circuitscape.org (accessed on 25 January 2022).
43. Li, H.Q.; Lian, Z.M.; Liu, X.L. The Status of Brown Eared Pheasant (Crossoptilon Manthurium) and Suggestions for Conservation. *J. Yanan Univ.* **2009**, *28*, 92–96.
44. Zhang, L.X.; Chen, X.L.; Xin, X.G. Short commentary on CMIP6 Scenario Model Intercomparison Project (ScenarioMIP). *Clim. Change Res.* **2019**, *15*, 519–525.
45. Ma, J.H. Habitat characteristics of brown eared pheasant and its conservation measures in the Heicha Mountains. *Shanxi Agric. Econ.* **2016**, *15*, 51. [CrossRef]
46. Peng, J.; Yang, Y.; Liu, Y.; Hu, Y.; Du, Y.; Meersmans, J.; Qiu, S. Linking ecosystem services and circuit theory to identify ecological security patterns. *Sci. Total Environ.* **2018**, *644*, 781–790. [CrossRef] [PubMed]